

Supporting Information

Natural Wood with Optimal Capillary Water Content and Evaporation

Enthalpy for Efficient Interfacial Solar Steam Generation

Maosong Tian^a, Junbo Chen^a, Jingfu Tian^a, Zhihao Liang^a, Yuanpeng Xie^{a,b*}

^aCollege of Materials and Metallurgy, Guizhou University, Guiyang, 550025 China.

^bSchool of Chemistry and Chemical Engineering, Guizhou University, Guiyang, 550025 China.

Email: ypxie@gzu.edu.cn

Supporting Notes

Note S1. Thermal Conductivity Characterization

The thermal conductivities of aerogels were measured via a heat resource method.¹ The wood samples, which were approximately 20 mm thick, were placed between two 10 mm glass plates to create a sandwich structure. This structure was then put onto a copper plate that had a stable heat source applied to it. Using the Fourier equation, the thermal conductivity (k) of the woods could be calculated.²

$$q'' = k \frac{dT}{dx} \quad \#(1)$$

Where q'' is the heat flux, and dT/dx is the temperature gradient of the section in the vertical direction.

The formula used to calculate the thermal conductivity of the konjac aerogel is as follows:

$$k_g \frac{dT_1}{dl_1} = k \frac{dT_2}{dl_2} \quad \#(2)$$

where k_g the thermal conductivity of glass ($1.05 \text{ W m}^{-1} \text{ K}^{-1}$). l_1 and l_2 are the thickness of the glass and sample, respectively. dT_1 and dT_2 are the temperature changes of the upper and lower surfaces of the glass and sample, respectively.

Note S2. Dark Evaporation test of Equivalent Evaporation Enthalpy

The equivalent evaporation enthalpy of water in the evaporator can be determined by comparing the evaporation flux of bulk water with that of the evaporator, assuming the same energy input (U_{in}) in the dark.³

$$U_{in} = E_{equ} m_g = E_0 m_0 \quad \#(3)$$

where E_0 and m_0 refer to the evaporation enthalpy and water mass change in the dark without evaporator, respectively, m_g is the water mass change using S-wood.

Note S3. Molecular Dynamics Simulation of Hydrogen bonding

The simulation cells with a size of $30 \text{ \AA} \times 30 \text{ \AA} \times 100 \text{ \AA}$ were set. Firstly, a script is used to construct a surface structure model of flat N-wood, E-wood, and S-wood.

Then, 240 water molecules are spread on the surface. Finally, the dynamics calculation begins using the NVT ensemble with a time step of 1 fs and a total simulation time of 1000 ps. The Dreiding force field is used to describe the van der Waals interactions between molecules, and the PPPM method is used to calculate the electrostatic interactions between molecules with a van der Waals truncation radius of 15.5 Å.

Supporting tables

Table S1. Price comparison of carbon black with other carbon materials.

Materials	Price (\$ kg ⁻¹)	Absorption (%)
Graphene oxide	24.65	92.5
Carbon nanotubes	16.43	99.0
Toner	11.64	98.6
Carbon black	0.37	97.8

Table S2. The cost estimation of raw materials in this work.

Chemicals	Price (\$ kg ⁻¹)	Reference
Sodium hydroxide	0.20	hnchg
Sodium sulphite	0.13	geeyeschem
Hydrogen peroxide	0.08	haihangchem
Dimethyl sulfoxide	0.14	geeyeschem
Formic acid	0.26	jnzshg
Acetic acid	0.27	qichenhg
1,3-Propanesultone	0.90	kangtuochem
Balsa wood	0.10	zhuhaidechi
Carbon Black	0.37	quanfeng
Total		6.6 \$ m ⁻²

Table S3. A comparison of our evaporator with other literatures

Device	Cost (\$ m ⁻²)	Evaporation rate (kg m ⁻² h ⁻¹)	Energy efficiency (%)	Ref.
HHE 3	14.9	3.2	90	4
RGO200/FeNi-	103.5	1.43	90.23	5

wood				
3D-GMN	382.17	2.71	95	6
TWA	9.29	1.17	-	7
PPy-paper	18	2.12	91.5	8
PCFE	13.5	1.7	94.6	9
PC@PDA-C	6.8	2.13	94.8	10
S-wood	6.6	3.37	97.2	Our work

Supporting Figures

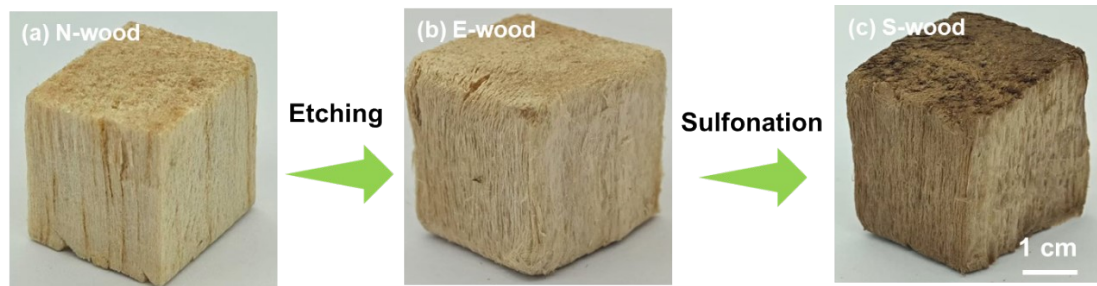


Fig. S1 The real photograph of three woods.

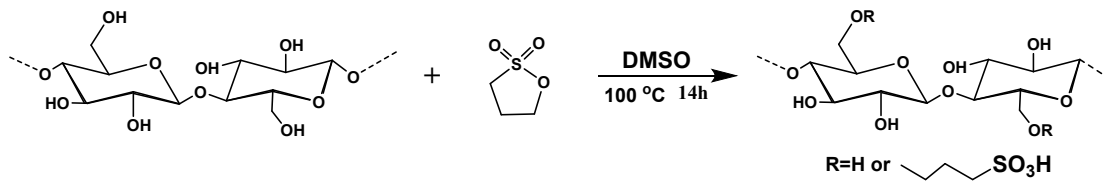


Fig. S2 The in-situ growth reactions of S-wood

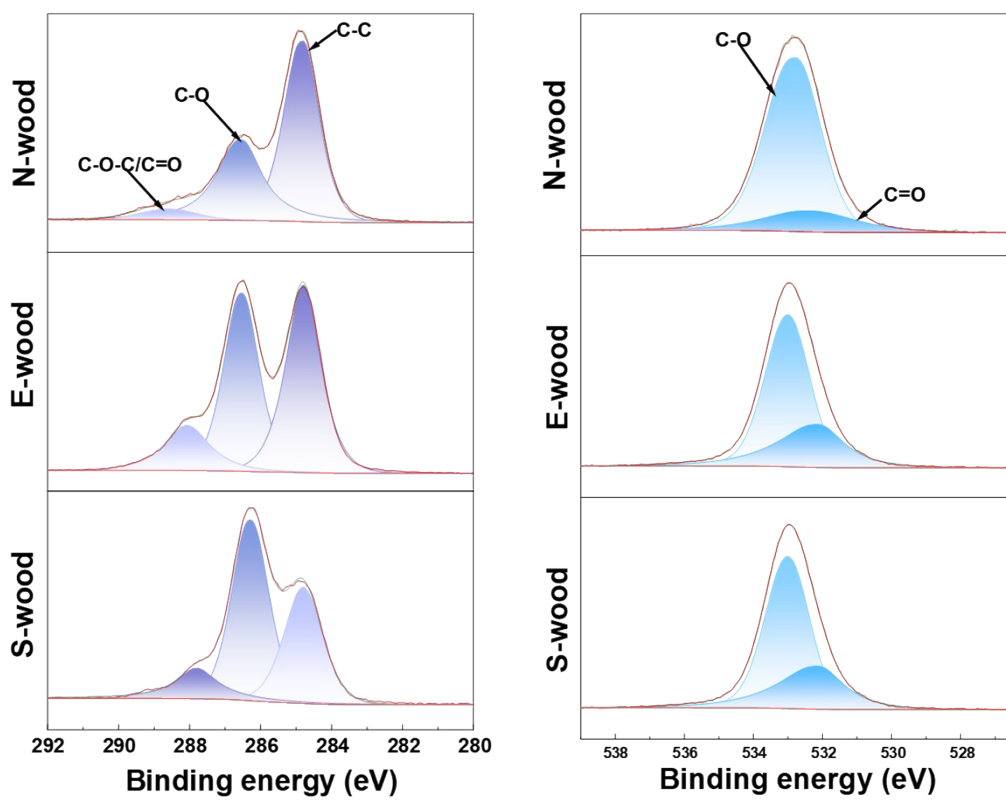


Fig. S3 XPS analysis of wood samples (N-wood, E-wood and S-wood). C 1s spectra (left) and O 1s spectra (right).

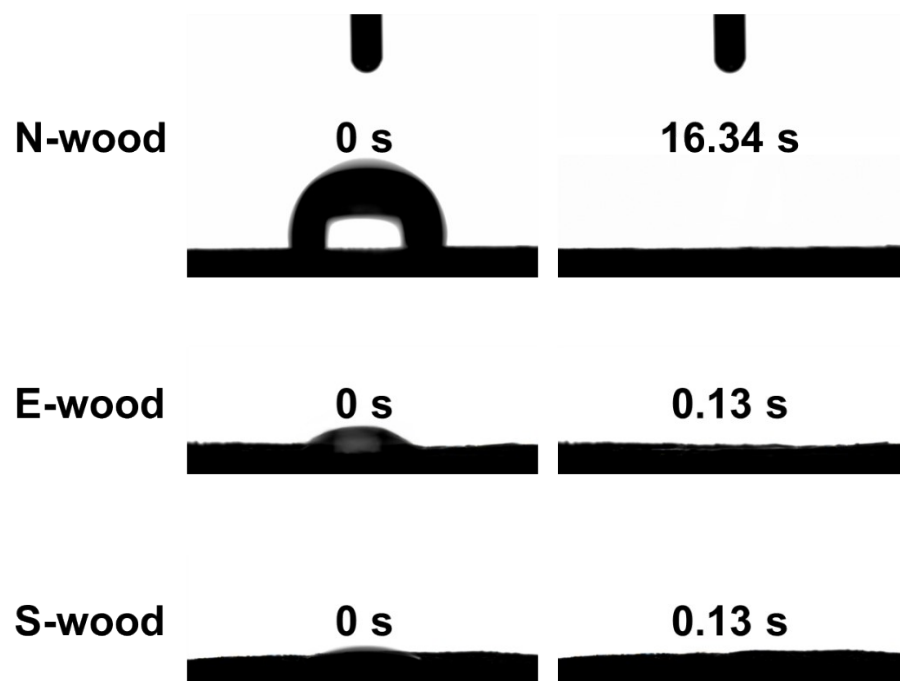


Fig. S4 The contact angle measurement of three samples.



Fig. S5 The mechanically robust and flexibility of S-wood.

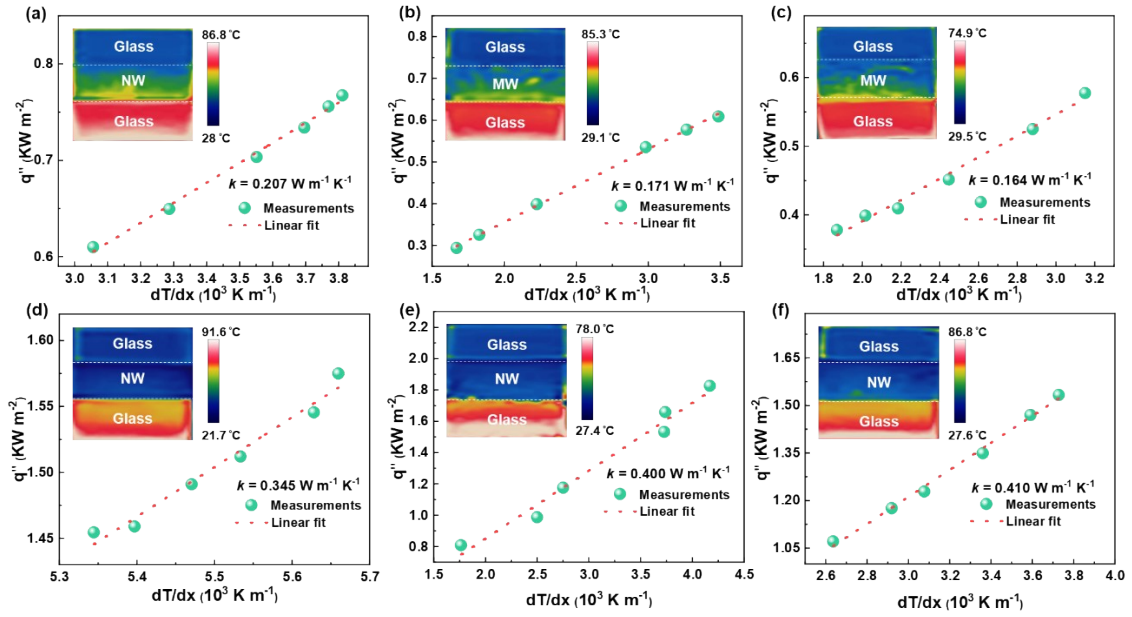


Fig. S6 The thermal conductivity of N-wood, E-wood, and S-wood in dry and wet structure state a-c) N-wood, E-wood, and S-wood, dry state, d-f) N-wood, E-wood, and S-wood, wet state. The inset figures are one of the representative pictures monitored by infrared camera.

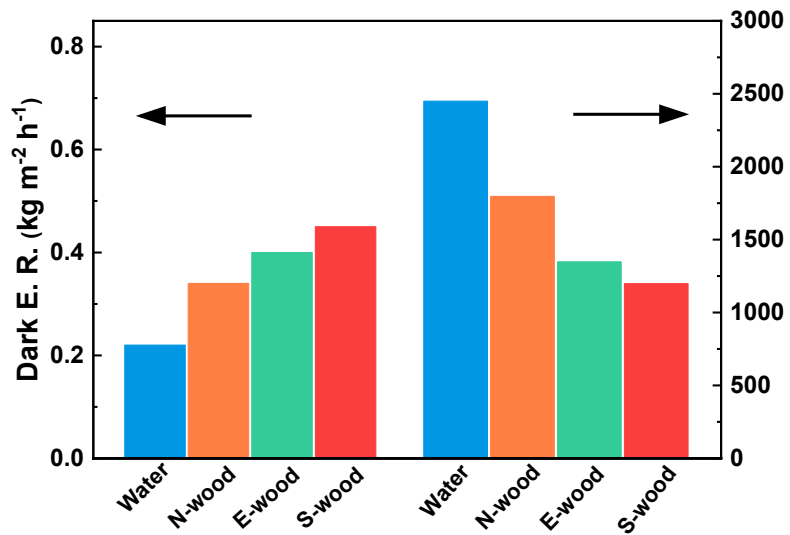


Fig. S7 Equivalent evaporation enthalpy result of N-wood, E-wood, and S-wood by dark evaporation test

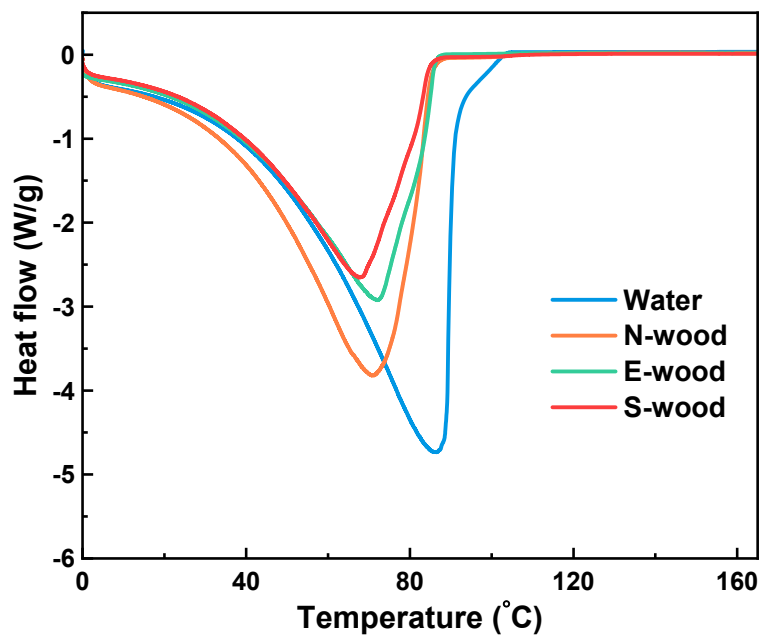


Fig. S8 Evaporation enthalpy result of N-wood, E-wood, and S-wood by DSC test

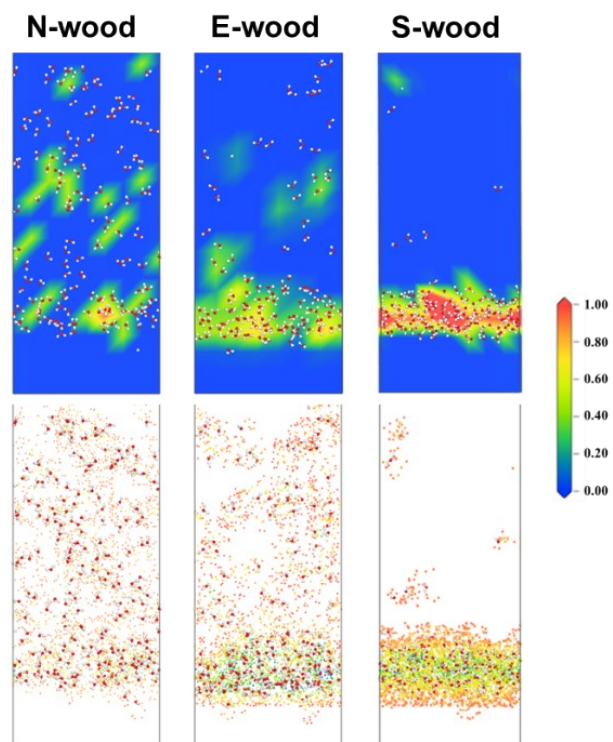


Fig. S9 The density distribution of the interfacial water molecules and the corresponding slices of N-wood, E-wood, and S-wood at 500 ps.

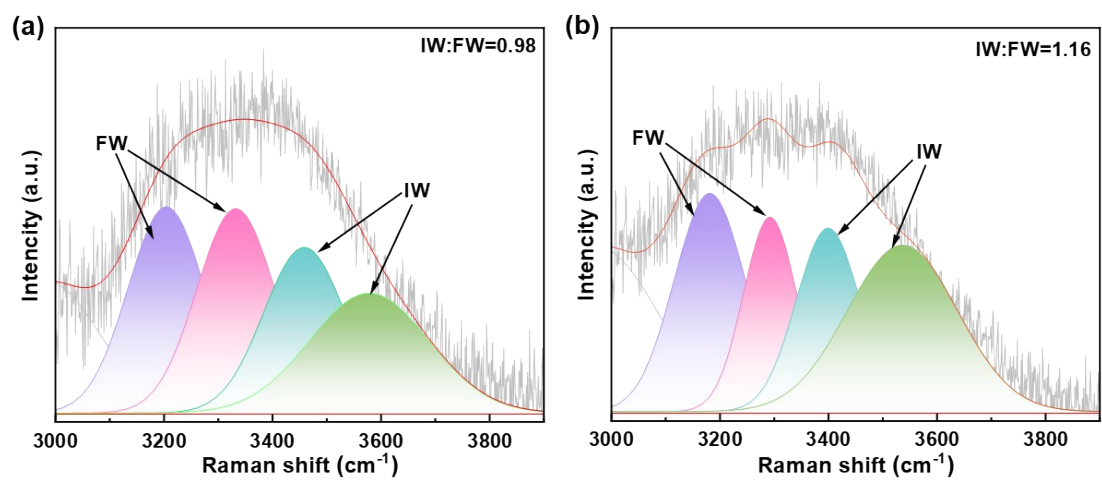


Fig. S10 Raman spectrum with fitting curves of (a) E-wood, (b) S-wood.

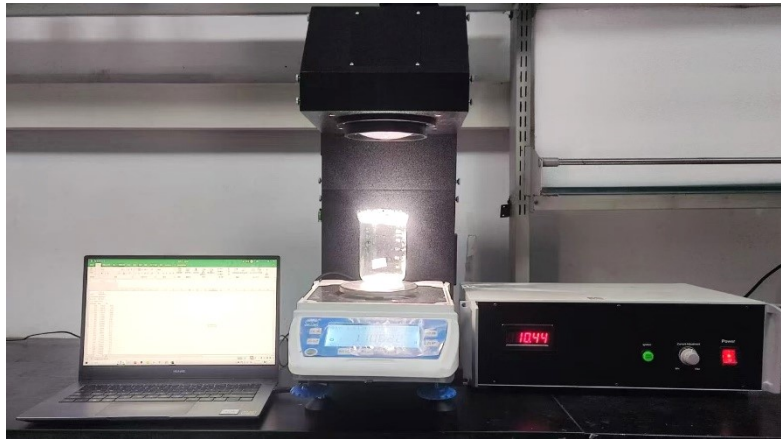


Fig. S11 The real picture of solar evaporator test system with a simulated 1.5 global (AM 1.5 G) solar irradiation.

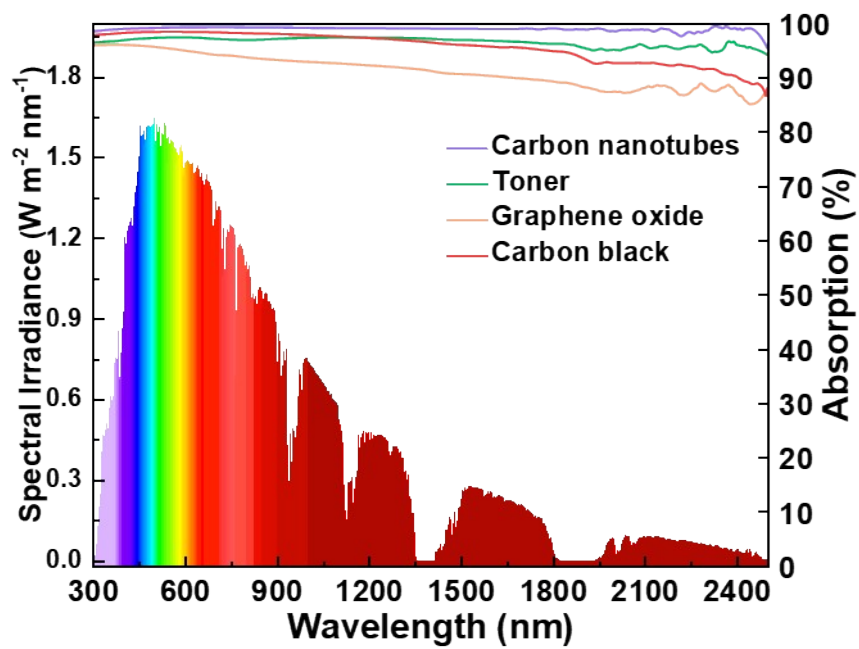


Fig. S12 AM1.5G solar spectrum and the absorption of Graphene oxide, Carbon nanotubes, Toner and Carbon black.

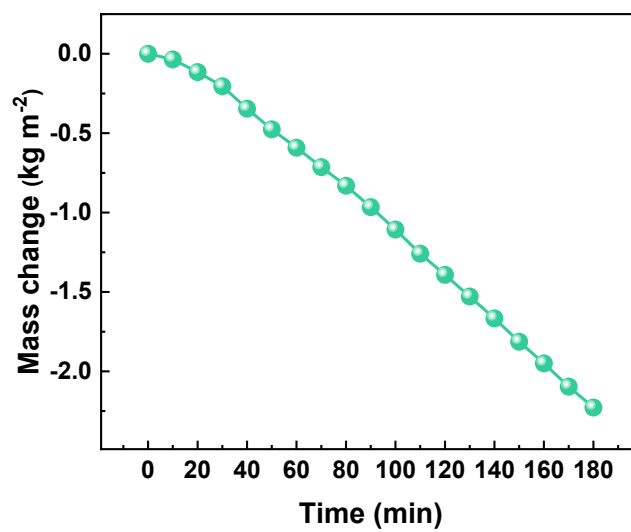


Fig. S13 The mass change curve of pure water.

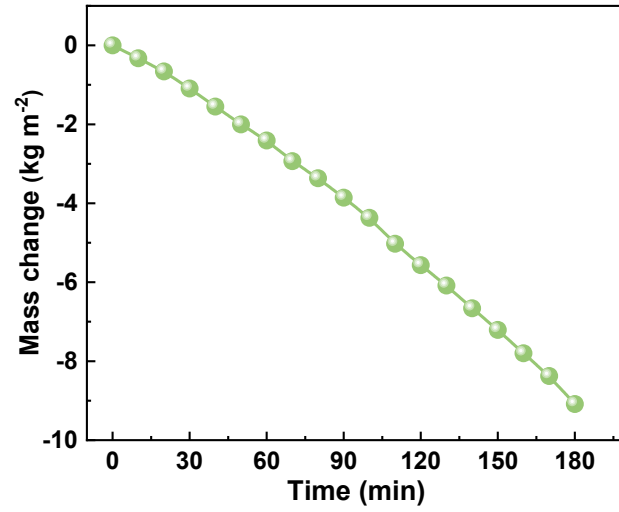


Fig. S14 The evaporation performance of S-wood under natural conditions of 53% humidity and a temperature of 25 °C.

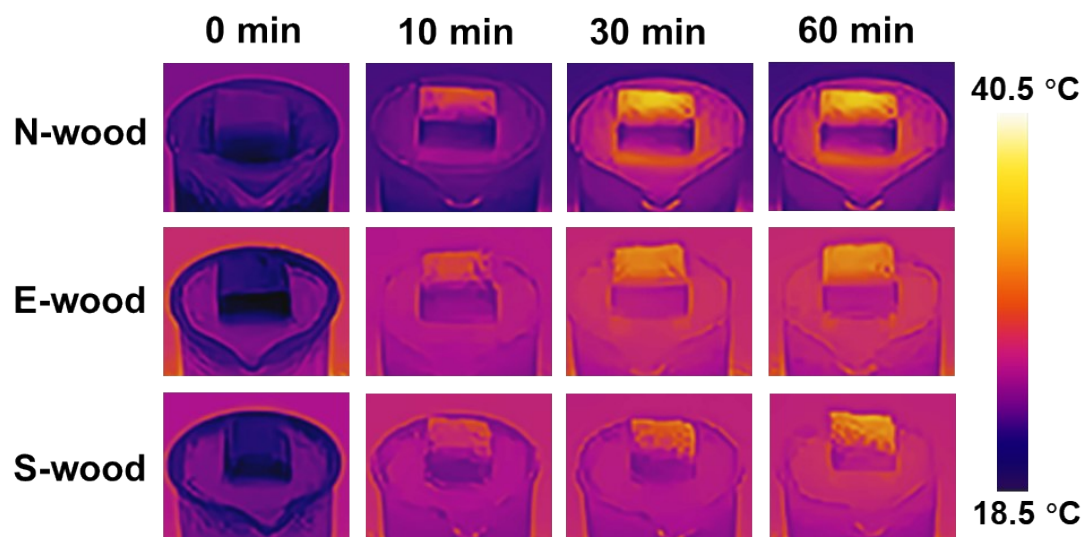


Fig. S15 The corresponding IR images of N-wood, E-wood, and S-wood within initial 60 min.

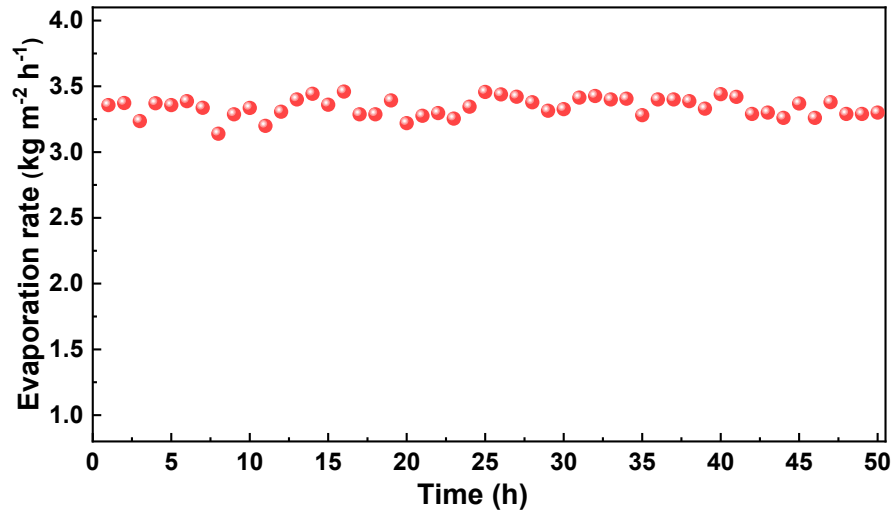


Fig. S16 The long-term evaporation performance of S-wood based ISSG.

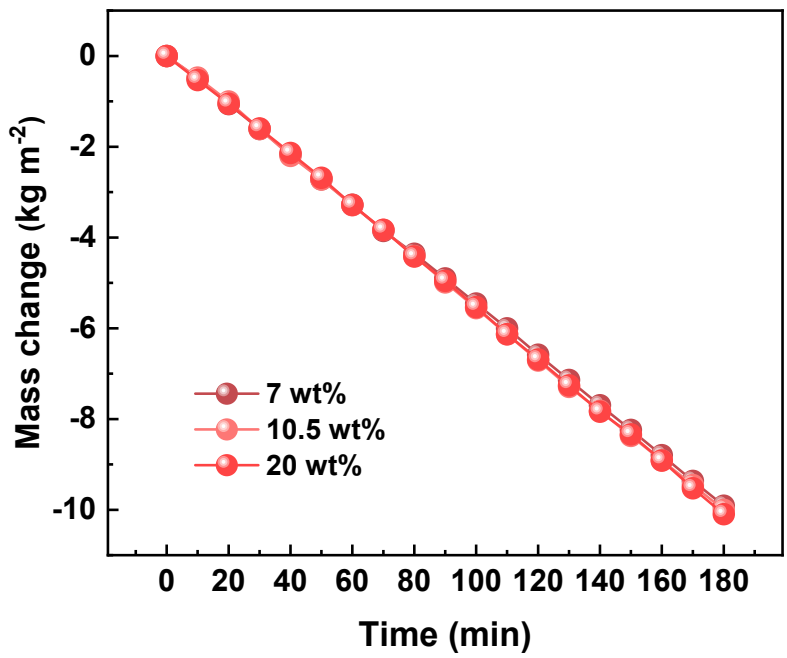


Fig. S17 The evaporation performance of S-wood in different concentrations of saline.

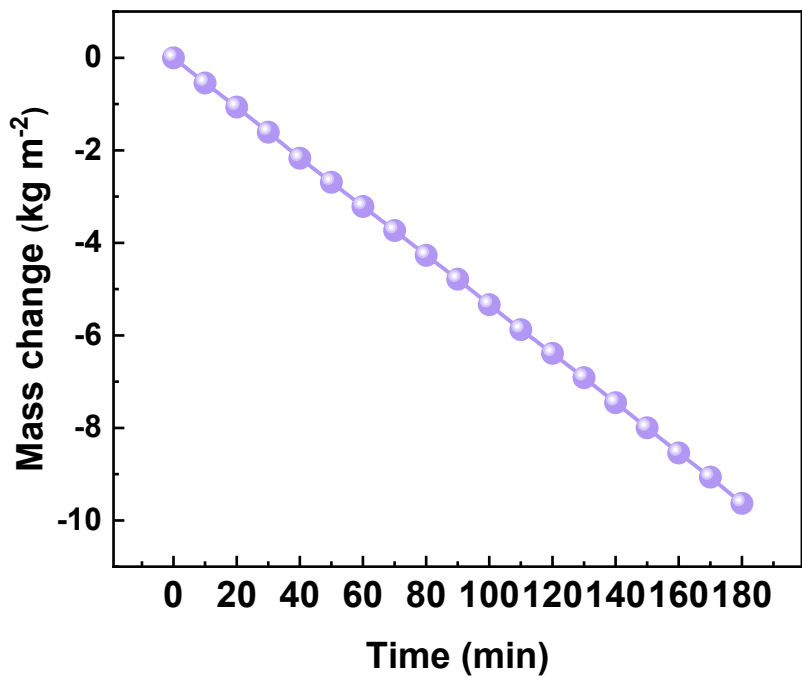


Fig. S18 The evaporation performance of S-wood in oil-water mixture.

References

1. J. Wan, A. Fan, H. Yao and W. Liu, *Energy Convers. Manage.*, 2015, **96**, 605-612.
2. H. Li, Y. He, Y. Hu and X. Wang, *ACS Appl. Mater. Interfaces*, 2018, **10**, 9362-9368.
3. Z. B. Wang, R. Y. Jin, S. Y. Zhang, X. Han, P. Guo, L. Jiang and L. P. Heng, *Adv. Funct. Mater.*, 2023, **33**, 2306806.
4. Y. Guo, H. Lu, F. Zhao, X. Zhou, W. Shi and G. Yu, *Adv. Mater.*, 2020, **32**, e1907061.
5. R. Mehrkhah, E. K. Goharshadi, M. M. Ghafurian, M. Mohammadi and O. Mahian, *Sol. Energy*, 2021, **224**, 440-454.
6. Y. Kong, H. Dan, W. Kong, Y. Gao, Y. Shang, K. Ji, Q. Yue and B. Gao, *J. Mater. Chem. A*, 2020, **8**, 24734-24742.
7. T. Meng, B. Jiang, Z. Li, X. Xu, D. Li, J. Henzie, A. K. Nanjundan, Y. Yamauchi and Y. Bando, *Nano Energy*, 2021, **87**, 106146.
8. W. Li, Z. Li, K. Bertelsmann and D. E. Fan, *Adv. Mater.*, 2019, **31**, e1900720.
9. G. Zhao, Y. Chen, L. Pan, B. Chen, L. Ren, X. Xiao, H. Yang and W. Xu, *Sol. Energy*, 2022, **233**, 134-141.
10. Y. Liu, H. Liu, J. Xiong, A. Li, R. Wang, L. Wang, X. Qin and J. Yu, *Chem. Eng. J.*, 2022, **427**, 131539.